

Strategies for the integration between FE Electronics and Detectors

Cardarelli Roberto
INFN sez. Tor Vergata

Introduction

New high-energy experiments in accelerator machines require particle detectors to have high counting capabilities, high time resolution and high spatial resolution. These requests have a major impact on the design of gas detectors and on the electronic front end

Increasing the counting capacity implies moving the amplification from the gas to the electronics which must have high gains and very low noise

Increasing the time resolution requires very rapid multiplication processes in the gas, very intense electric fields, and fast electronics and the measurement of the signal Amplitude for the correction of the rising time

Comparison: solid state detectors v.s. gas detectors evolution

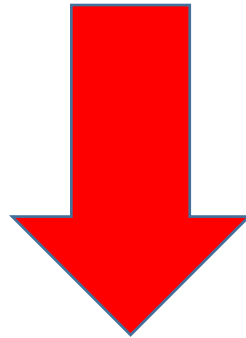
Solid state detectors

- no gain
- low gain

gas detectors

high gain

low gain



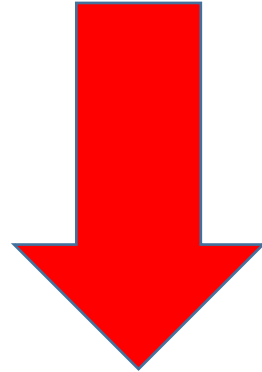
Time resolution evolution

Solid state detectors

- mm thickness

gas detectors

radial electric field

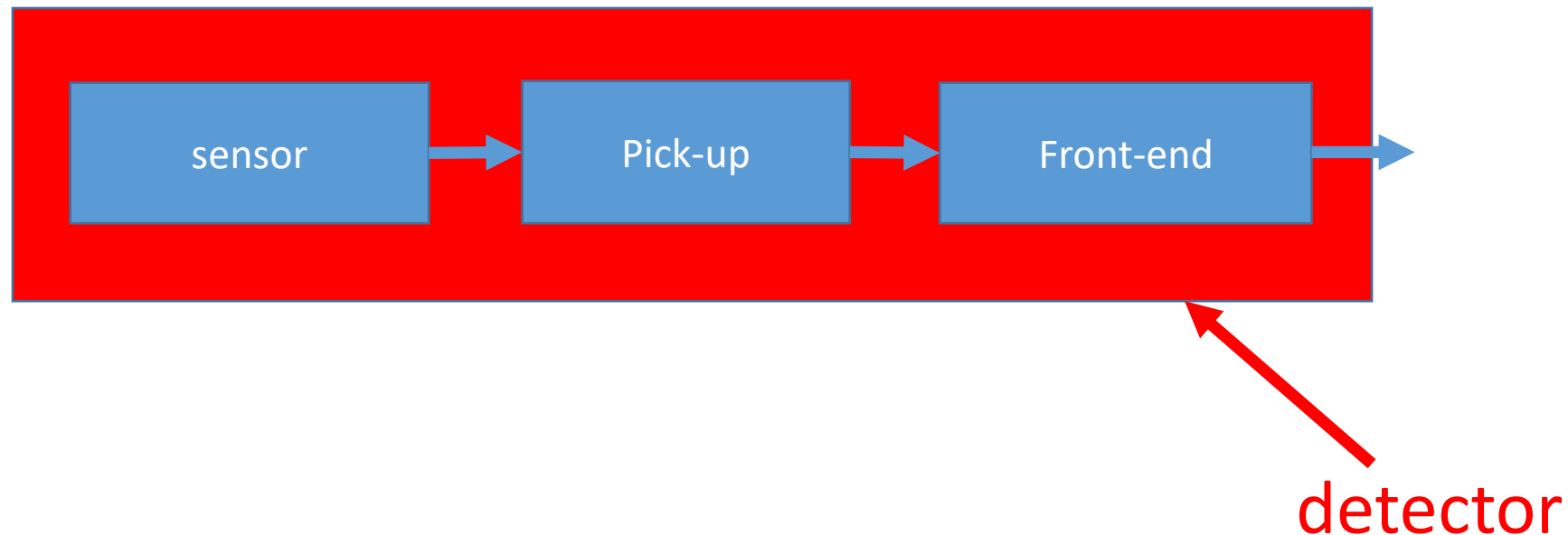


- Low thickness

uniform electric field

Front End – Detector integration

From what has been said it can be deduced that the detector and the front-end electronics are so interconnected that they must be considered as a single block and therefore the integration of the detector and the electronics assumes a fundamental role.



Connection between detector and front-end

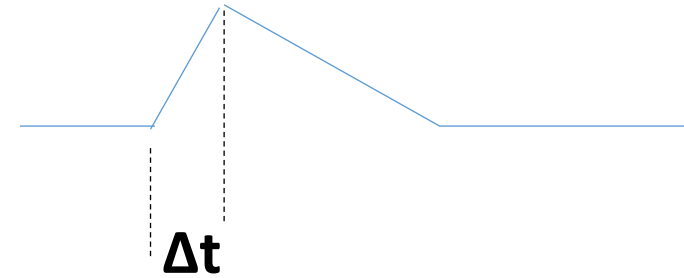
The connection between the detector and the front-end is made through the pick-up which must simultaneously satisfy two needs:

- to maximize the collection of charges produced in the detector(Ramo's theorem)
- to transfer the signal to the front-end without distortion.

Pick-up normally used

$$\lambda = \Delta t * c$$

c=propagation velocity



Pad $\lambda > L$



capacitive adaptation

Strip-line $\lambda < L$



resistive adaptation

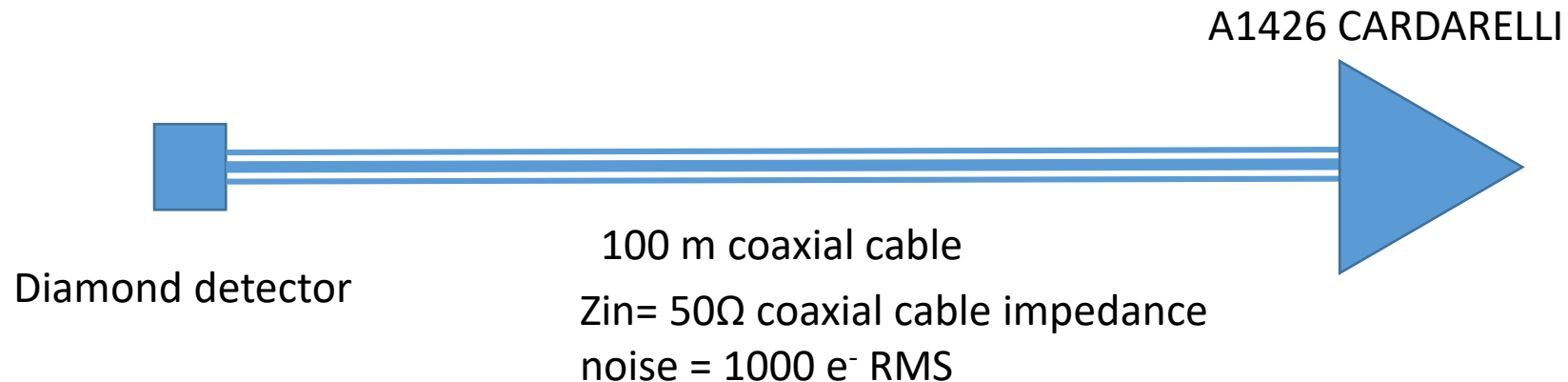
Noise considerations

Equivalent capacity calculation to evaluate electronic noise

Pad → $C=K*L^2$

strip-line → $C=K*\lambda$

Test

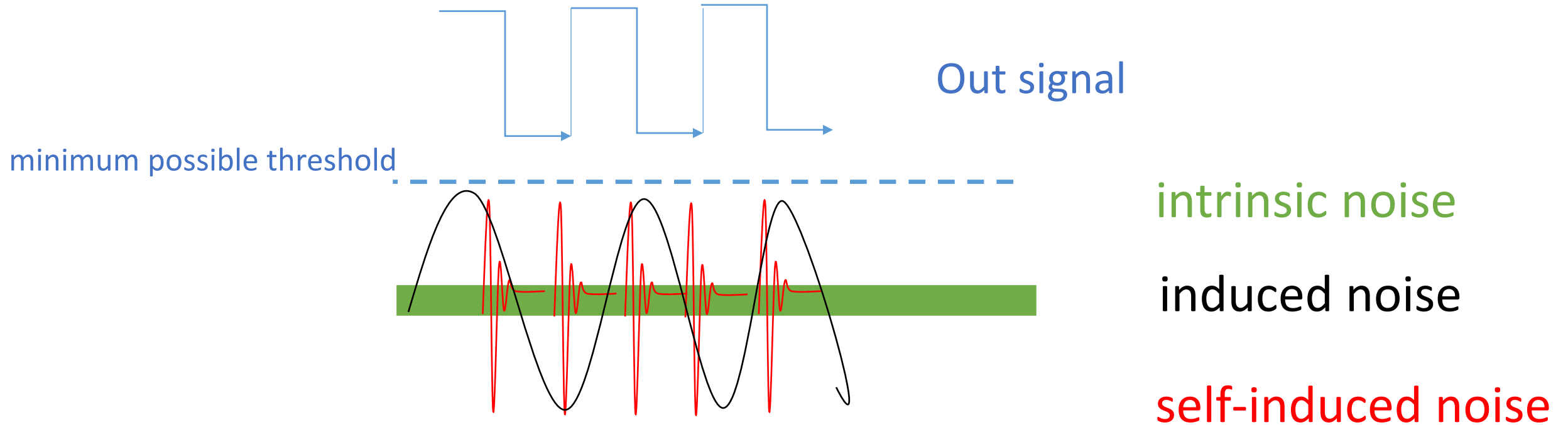


Noise considerations

Electronic noise can be summarized as composed of three types:

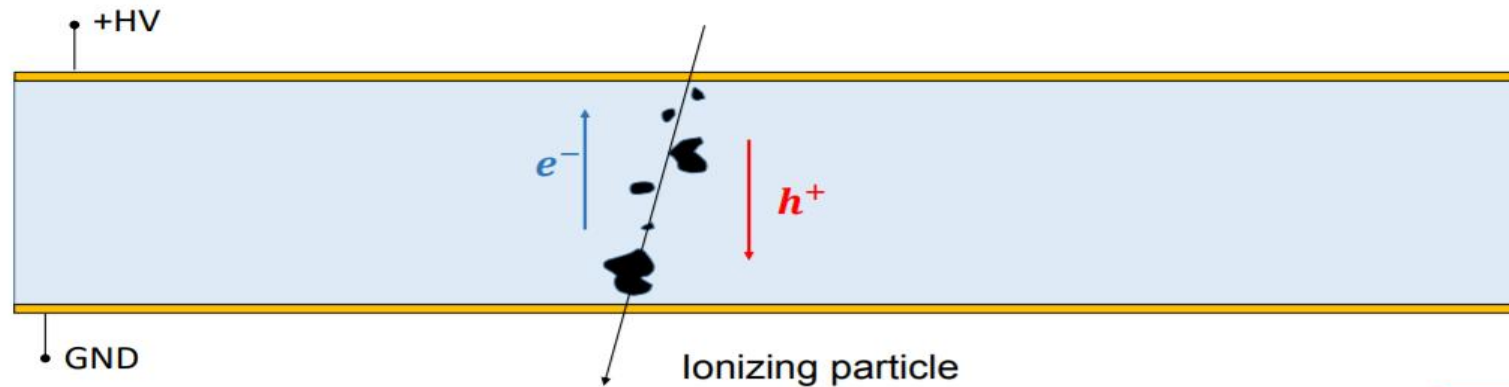
- 1) **intrinsic noise** (Johnson, $1/f$, ... , Noise) **unavoidable**
- 2) **induced noise** (radiofrequency, Noise) **Faraday's cage**
- 3) **self-induced noise** (common mode current noise produced by low impedance output signals) **differential signals, ground connections**

Forms of the different types of noise



Landau noise

2. Charge-collection (or Landau) noise



is produced by the **non uniformity of the charge deposition** in the sensor:

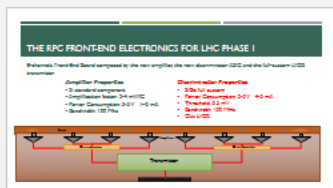
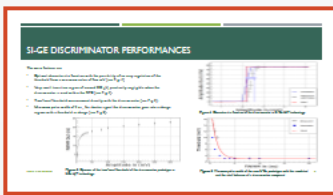
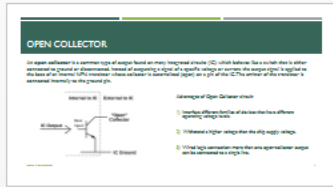
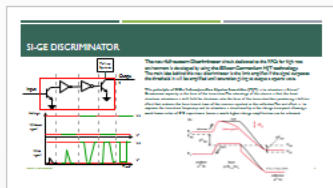
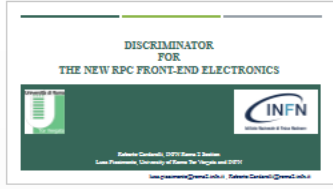
$$I_{ind} \cong v_{drift} \frac{1}{D} \sum_i q_i$$

When **large clusters** are absorbed at the electrodes, their contribution is removed from the induced current. The **statistical origin** of this variability of I_{ind} makes this **effect irreducible** in PN-junction sensors.

Minimum possible threshold

Once induced and self-induced noises have been eliminated, the number of spurious signals produced by the discriminator are:

- $V_{th} = n\sigma$ $F = P(n\sigma) * BW$
- **F** frequency of false pulses discriminator from noise
- **P(nσ)** probability of having a higher tension ($n * \sigma$ noise)
- **BW** passband amplifier



SI-GE DISCRIMINATOR PERFORMANCES

The main features are:

- Optimal characteristic function with the possibility of an easy regulation of the threshold from a minimum value of few mV (see Fig. 4)
- Very small transition region of around 300 μ V, practically negligible when the discriminator is used within the RPC: (see Fig 4).
- Time-over-threshold measurement directly with the discriminator (see Fig 5).
- Minimum pulse width of 3 ns ; for shorter signal the discriminator goes into a charge regime with a threshold in charge (see Fig 6).

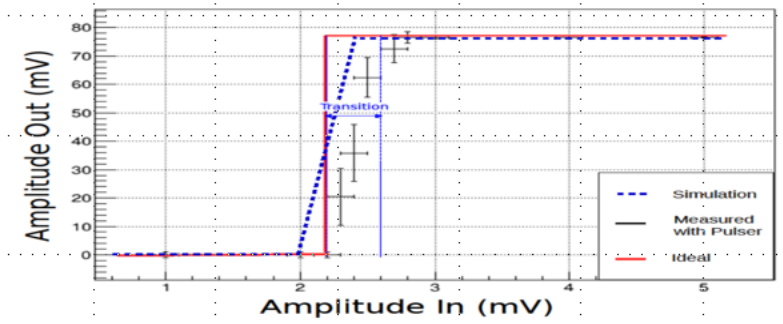


Figure 4: Characteristic function of the discriminator in Si-Ge HJT technology

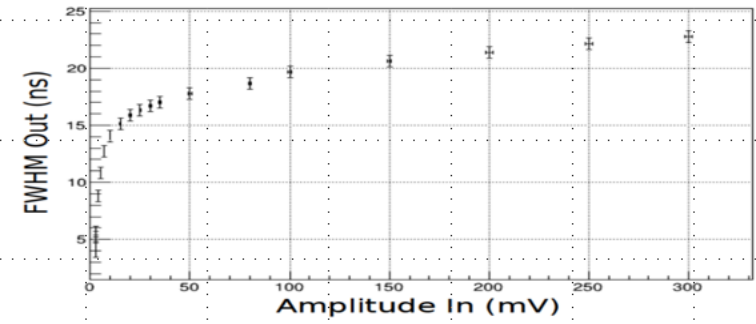


Figure 5: Dynamic of the time-over-threshold of the discriminator prototype in SiGe HJT technology:

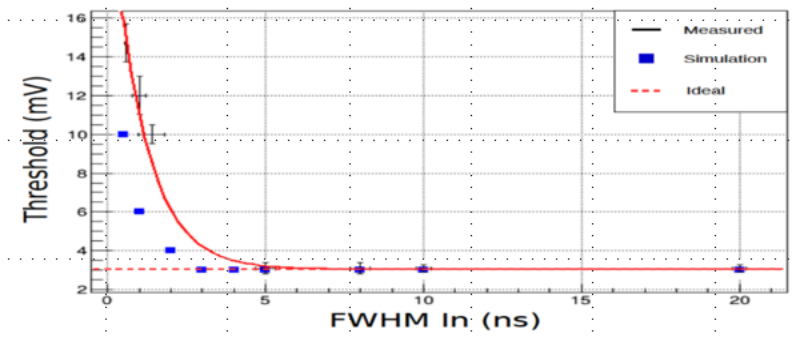


Figure 6: Minimum pulse width of the new Si-Ge prototype with the simulated and the ideal behavior of a discriminator compared

LUCA PIZZIMENTO

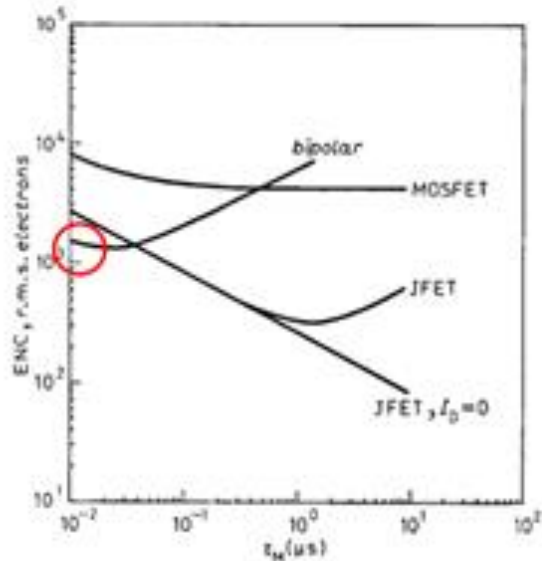
Low noise amplifier



The fast, low noise amplifier

$$ENC^2 \propto \left(2q_e I_C + \frac{4kT}{R_P} + i_{na}^2 \right) \cdot \tau + \boxed{(4kTR_S + e_{na}^2) \cdot \frac{C_{in}^2}{\tau}} + 4A_f C_{in}^2$$

Dominating term: series noise (for TT-PET $\tau < 10$ ns)



Fast integrator

➔ Minimization of series noise

➔ Low input impedance of the transistor

➔ BJT technology

BJT Si v.s. SiGe

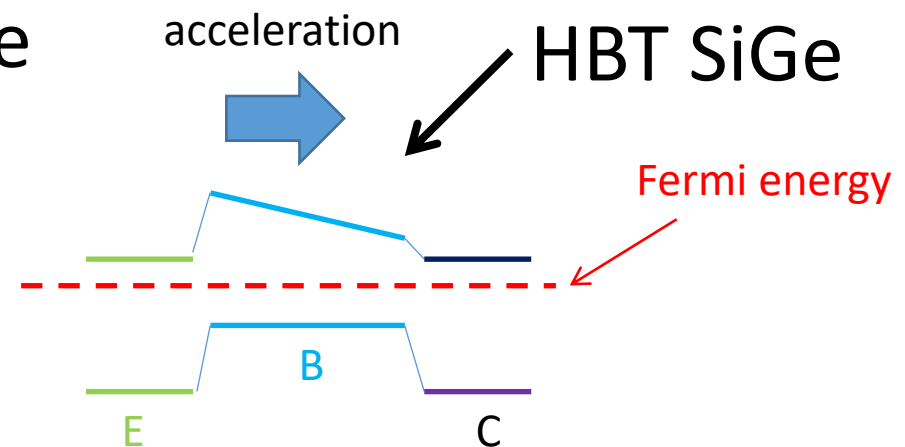
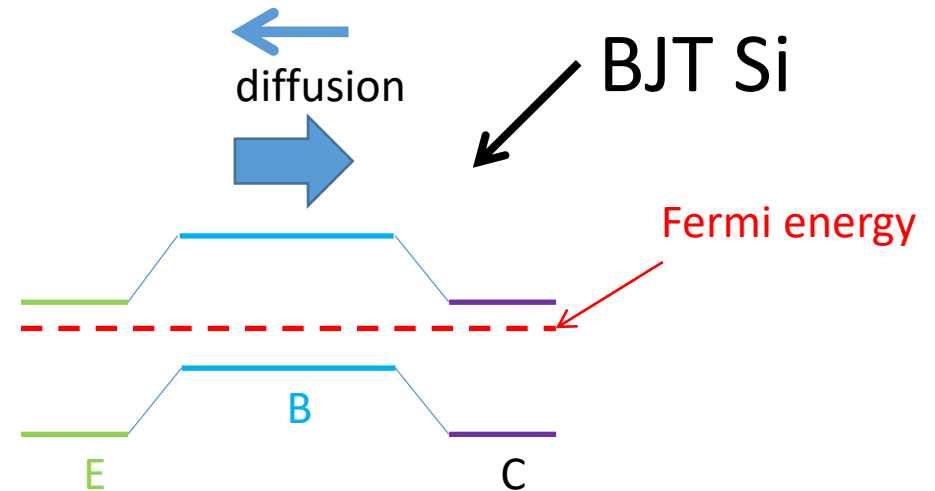
BJT performances

- $\beta = \tau_c / \tau_t$
- $f_t = 1 / \tau_t$
- $N = K * \tau_t$

τ_c = hole recombination time in Base

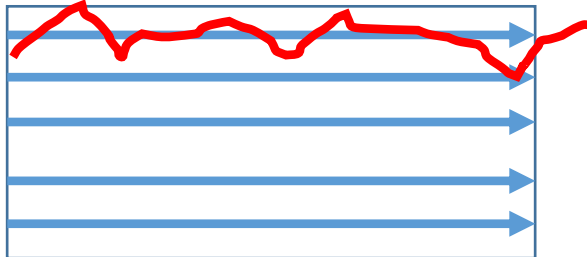
τ_t = base transient time

τ_t (Si) \gg τ_t (SiGe)



Comparison BJT v.s. HBT SiGe

$F_t = 350 \text{ GHz}$ $\beta = 900$



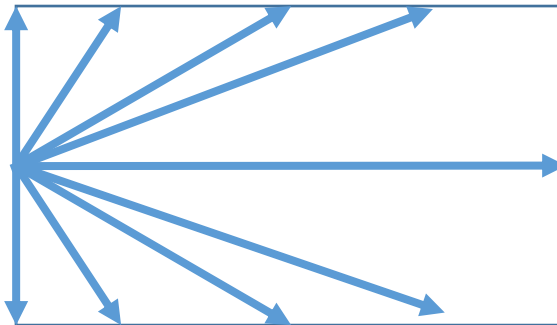
HBT SiGe

E

B

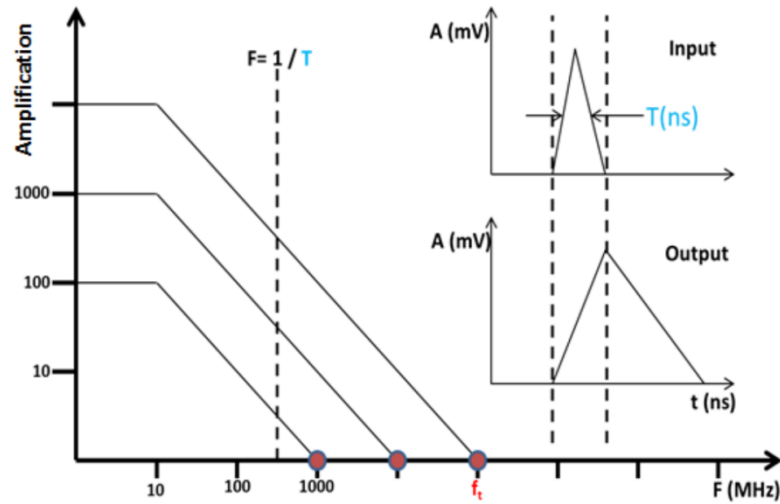
C

$F_t = 10 \text{ GHz}$ $\beta = 30$



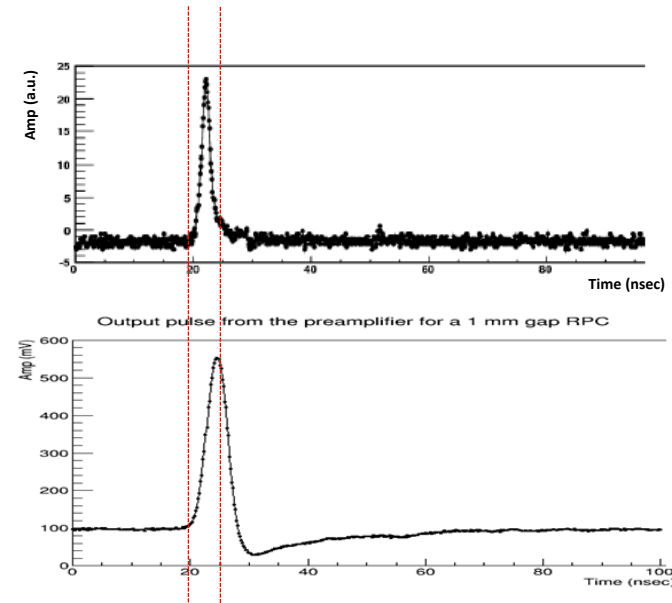
BJT

Strategy for the new front-end (SiGe)

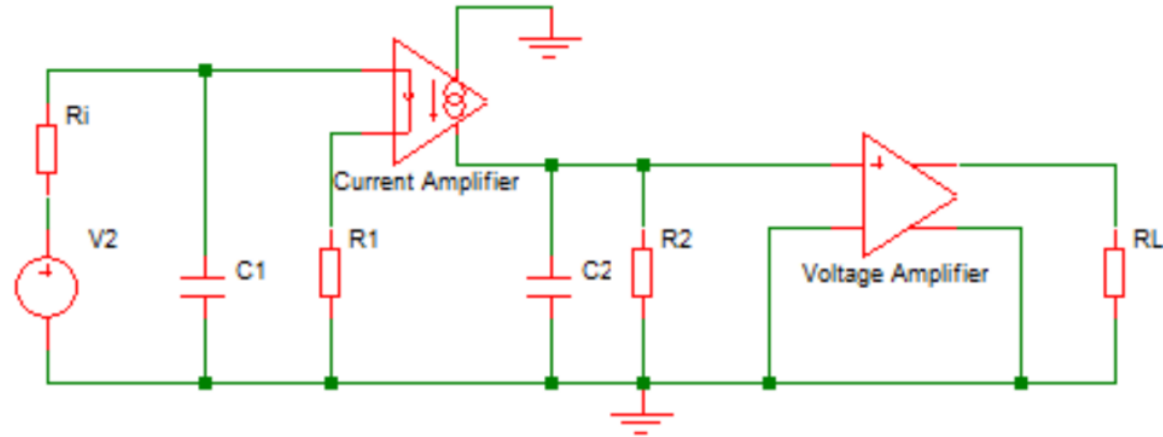


Working strategy

Actual result for
the RPC signal



The block diagram of the preamplifier



The same scheme can be used for both Silicon and SiGe technology for a comparison.

Silicon technology

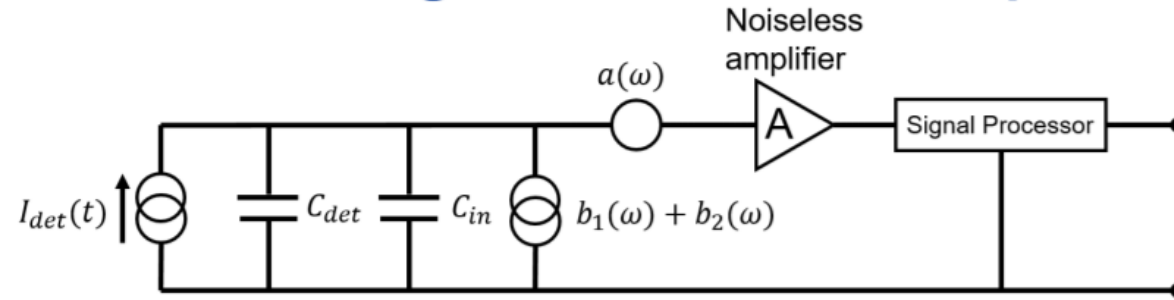
Voltage supply	3–5 Volt
Sensitivity	2–4 mV/fC
Noise (independent from detector)	4000 e^- RMS
Input impedance	100–50 Ohm
B.W.	10–100 MHz
Power consumption	10 mW/ch
Rise time $\delta(t)$ input	300–600 ps
Radiation hardness	1 Mrad, 10^{13} n cm^{-2}

SiGe technology

Voltage supply	2–3 Volt
Sensitivity	2–6 mV/fC
Noise (independent from detector)	500 e^- RMS
Input impedance	50–200 Ohm
B.W.	30–100 MHz
Power consumption	2 mW/ch
Rise time $\delta(t)$ input	100–300 ps
Radiation hardness [4]	50 Mrad, 10^{15} n cm^{-2}

Noise v.s. β and R_b

Equivalent Noise Charge: device comparison



$$ENC^2 = A_1 \frac{a_W}{\tau_M} (C_{det} + C_{in})^2 + A_2 \frac{\ln 2}{\pi} c (C_{det} + C_{in})^2 + A_3 (b_1 + b_2) \tau_M$$

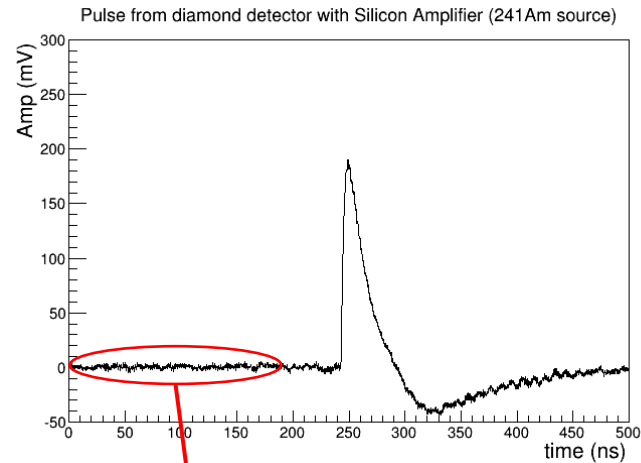
BJT based amplifier

$$ENC_{\text{series noise}} \propto \sqrt{k_1 \cdot \frac{C_{tot}^2}{\beta} + k_2 \cdot R_b C_{tot}^2}$$

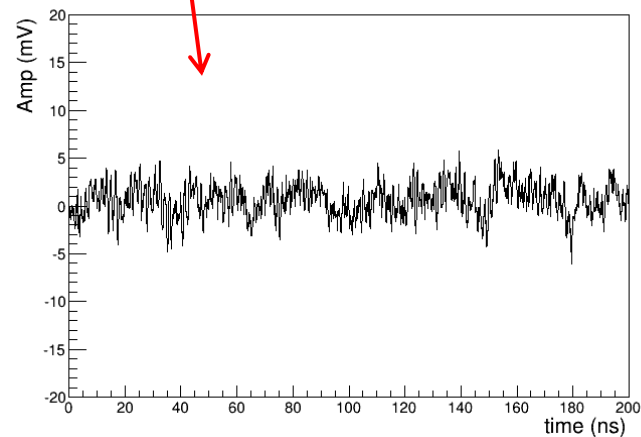
Signal and noise from SiGe Amplifier and Silicon Amplifier

Pulses recorded from a 500 micron diamond sensor irradiated by ^{241}Am source.

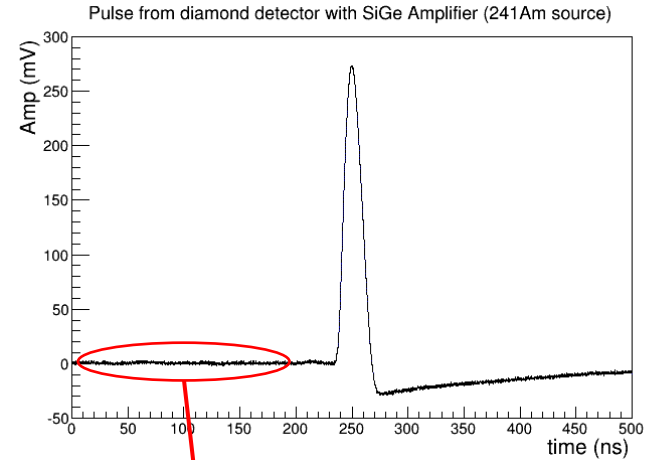
Silicon amplifier



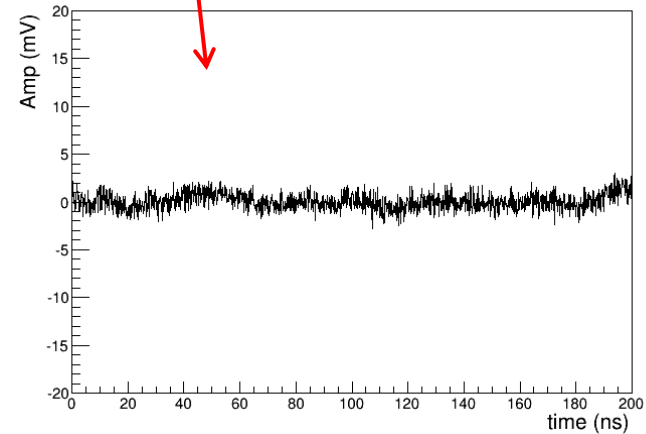
Noise from Silicon Amplifier



SiGe amplifier



Noise from SiGe Amplifier



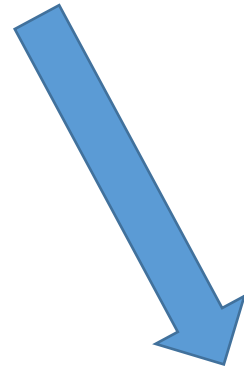
CMOS and HBT comparison

CMOS

high density low consumption

HBT

high frequency analog
circuits low noise

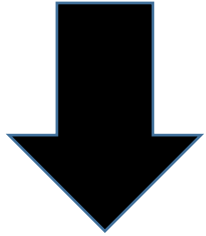


BiCMOS

Possible developments

BiCMOS

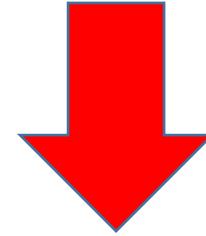
- 60 nm $\beta=900$ $F_t=350\text{GHz}$ today



- 20 nm $\beta=1500$ $F_t=1\text{ THz}$ next years

CMOS

20nm



10-7 nm

- BCMOS high flexibility and high development potential
- CMOS development limit of atom size, difficulty in making precise simulation models

Conclusions

Given the high performance required for the gas detectors in future experiments, the integration between the detector and the front-end electronics acquires a fundamental importance. The choice of technology must be made by rewarding flexibility and the possibility of development, for these reasons we recommend BiCMOS.